 ©2014 Kvantovaya Elektronika and Turpion Ltd

PACS numbers: 87.64.Cc; 87.63.L–; 78.67.Bf
DOI: 10.1070/QE2014v044n08ABEH015494

Study of contrasting properties of nanoparticles for optical diffuse spectroscopy problems

A.D. Krainov, P.D. Agrba, E.A. Sergeeva, S.V. Zabotnov, M.Yu. Kirillin

Abstract. **The results of experimental studies of the optical properties of gold and silicon nanoparticle suspensions and their use as contrasting agents in optical diffusion spectroscopy (ODS) are presented. The optical properties of nanoparticle suspensions and model media were reconstructed based on the data of spectrophotometry measurements in the range 500–1100 nm using an original theoretical model. The experimental studies using the ODS system were performed in a liquid phantom on the basis of the solution of lipofundin and Indian ink, modelling the optical properties of a real biotissue. The enhanced contrast of images, obtained using the ODS method in the experiments with the chosen suspensions of nanoparticles confirm the assumption about high potentialities of using them as contrast agents for the ODS problems.**

Keywords: *nanoparticles, contrasting, spectrophotometry, optical diffusion spectroscopy.*

1. Introduction

At present the method of optical diffuse spectroscopy (ODS) using cw radiation in the wavelength range 650–1200 nm is actively developed for noninvasive functional diagnostics and imaging of the inner structure of biological objects. The method is based on the detection of probing light diffusely scattered by the object of study at several wavelength, determined by the absorption spectra of the studied biotissue components [1]. An obvious advantage of this method is the simplicity of implementing the diagnostic tools that do not require fast sources and detectors of radiation, as well as high-frequency devices for signal processing. The main medical applications of the ODS method are the diagnosis of the oxygenation status of breast cancer tumours and the monitoring of the cerebral cortex activity (see, e.g., [1–3]). However, the essential drawbacks of this method are low resolution and contrast, as compared to the methods of optical coherence tomography or computed tomography, which may be critical when performing medical diagnostics.

A.D. Krainov, P.D. Agrba, E.A. Sergeeva, M.Yu. Kirillin Institute of Applied Physics, Russian Academy of Sciences, ul. Ul'yanova 46, 603950 Nizhnii Novgorod, Russia; N.I. Lobachevsky Nizhnii Novgorod State University, prosp. Gagarina 23, 603950 Nizhnii Novgorod, Russia; email: mkirillin@yandex.ru;
S.V. Zabotnov Department of Physics, M.V. Lomonosov Moscow State University, Vorob'evy gory, 119991 Moscow, Russia

Received 14 March 2014; revision received 15 June 2014
Kvantovaya Elektronika **44** (8) 757–762 (2014)
Translated by V.L. Derbov

The increased informativity of images, obtained by means of optical bioimaging methods, is implemented by using the clearing (e.g., glycerol or glucose solution) [4–7] or contrasting (gold, silicon, or organic nanoparticles) [8–21] agents that allow local control of the object optical parameters (scattering and absorption coefficients), which leads to contrasting the regions in the diagnostic images.

The promising applications of gold nanoparticles are associated with their low cytotoxicity and the possibility of essential variation of the object optical properties even at relatively low concentrations [8, 14, 19]. The use of gold nanoparticles allows a partial solution to the problem of early diagnosis of malignant neoplasms and their localisation, as well as development of new methods of selective (targeted) therapy by local heating of the metallic nanoparticles with IR laser radiation aimed at the thermal damage of the adjacent cells [15–18, 20–22].

In Ref. [9] the possibility of using polypirol nanoparticles as contrasting agents in OCT is considered. Experimental studies of nanoparticles in biotissue phantoms and calculations on the basis of Mie theory are also reported there.

Silicon nanoparticles seem not less promising for the diagnostics of living objects. Thus, e.g., in Ref. [12] the photoluminescence of porous silicon is studied. The photoluminescence spectrum of nanocrystals, forming this material, lies in the range from 700 to 900 nm, which determines high potential of their use in biomedical applications. It is also demonstrated that in contrast to carbon, gold particles, or quantum dots, the silicon nanostructures possess small (not exceeding 4 hours) time of decay into non-toxic components in living organisms.

Thus, the use of nanoparticles for increasing the informativity of images, obtained by means of bioimaging techniques, is urgent, since, on the one hand, it allows the improvement of their diagnostic value, and, on the other hand, it offers wide opportunities for theranostics, in which therapeutic facilities simultaneously serve as diagnostic tools.

The aim of the present paper is to study the possibility of using gold and silicon nanoparticles for enhancing the contrast of images, obtained using the ODS method.

2. Materials and methods

2.1. Objects of study

As contrasting agents we studied gold nanoparticles of arbitrary shape with characteristic size 30–100 nm (type 1), gold nanoparticles of arbitrary shape with a minor content of nanorods of length 30–50 nm and thickness 10–17 nm (type 2), pure gold nanorods of length 30–50 nm and thickness 10–17 nm (type 3) (fabricated at the Institute of Chemical

Physics, Russian Academy of Sciences, Moscow [22]) and silicon nanoparticles with a characteristic size 50–200 nm (type 4) (fabricated at the M.V. Lomonosov Moscow State University [23]).

In our work we also used the liquid phantom on the basis of lipofundin with the volume concentration 1.4% [24], the scattering properties of which correspond to the average indicators for mouse biotissue. The phantom was placed in the cuvette with the dimensions $16 \times 16 \times 4$ cm that corresponds to a typical volume of a biological object studied using the ODS method. The contrasted volume inside the object was modelled by a cylindrical test tube with the diameter 0.7 cm (the volume 0.65 mL), made of matted plastic and filled with the phantom. The control of optical properties of the studied volume was implemented by adding the nanoparticles suspension to the test tube.

To estimate numerically the ODS image contrast versus the coefficient of absorption, enhanced by the presence of a contrasting agent in the selected volume, we also performed the experiment in which instead of nanoparticle suspension the test tube was filled with Indian ink in different concentrations, which is characterised by a weak wavelength dependence of the absorption coefficient in the near IR range [24].

2.2. Determination of optical properties of nanoparticle suspensions

Optical properties of nanoparticle suspensions were determined basing on measuring the collimated transmittance (C), full transmittance (T) and full reflectance (R) using the spectrophotometry method. The spectrophotometric measurements were performed in the range 500–1100 nm using an Analytik Jena SPECORD 250 Plus spectrophotometer with an integrating sphere. The studied samples were placed into silica cuvettes 1, 5 and 10 mm thick, depending on the sample optical density, to provide the validity of the used model. It should be noted that in the process of measuring the full reflectance the sample was oriented at an angle slightly different from 90° to the probe beam axis to avoid recording the direct Fresnel reflection of the probing beam from the sample surface. The scattering and absorption coefficients of nanoparticle suspensions were determined by using the spectrophotometry data.

At present there are two classes of techniques aimed at determining optical characteristics of scattering and absorbing (turbid) media on the basis of spectrophotometry data, namely, the analytical and the numerical ones. Since generally the equation of radiation transport in turbid media has no exact solution, the analytical techniques are based on various approximations, namely, the Lambert–Bouguer–Beer law, the Kubelka–Munk theory, and the diffusion approximation of the radiation transport equation [25, 26]. However, the field of their application is essentially limited. The Lambert–Bouguer–Beer law yields only the sum of absorption and scattering coefficients, provided that the multiple scattering in the sample is absent, while the Kubelka-Munk theory and the diffusion approximation, on the contrary, are applicable only in strongly scattering media and do not allow for the presence of the collimated component. Moreover, the Kubelka–Munk theory does not correctly allow one to take into account the reflection and refraction of the diffusely scattered radiation at the boundaries of the silica cuvette used in the spectrophotometric studies of colloids and suspensions. An alternative approach is presented by the numerical technique based on the inverse Monte Carlo method, in which for each wavelength the optical characteristics are determined iteratively by means of the Newton method based on the modelling of radiation propagation in a turbid medium. The use of Monte Carlo method allows for both collimated and diffuse component of the radiation, scattered by the sample; however, it requires considerable computational facilities, i.e., is time-consuming.

In the present work in order to determine the optical characteristics of the studied suspensions of nanoparticles we used the technique based on the new hybrid analytical model (modified Lambert–Bouguer–Beer law) that allows for the collimated and diffuse components of the radiation, scattered by the sample, as well as the reflection and refraction of the scattered radiation at the boundaries of the silica cuvette. This makes it applicable to a wide class of samples with different optical properties and allows one to avoid time-consuming calculations required for the inverse Monte Carlo method.

The considered model [27] is based on representing the scattering coefficient μ_s as a sum of two components, μ_{fs} and μ_{bs}, responsible for scattering into the front and back semispace, respectively:

$$\mu_s = \mu_{fs} + \mu_{bs}. \tag{1}$$

In this case one can consider the scattering coefficient μ_{bs} to be responsible for the attenuation of the radiation passed through the medium, while the scattering coefficient μ_s is responsible for the attenuation of its collimated component. Then in the low-order scattering approximation ($\mu_s d < 1$) with the attenuation due to the absorption in correspondence with the Lambert–Bouguer–Beer law for collimated and full transmission we get

$$C = T_F^2 \exp[-(\mu_s + \mu_a)d], \tag{2}$$

$$T = T_F^2 \exp[-(\mu_{bs} + \mu_a)d], \tag{3}$$

where d is the thickness of the medium layer; μ_a is the absorption coefficient; $T_F = 4n/(n+1)^2$ is the Fresnel transmission coefficient for the radiation, normally incident on the boundary of the medium; and n is the medium refractive index.

Next, the reflection from each infinitely thin layer with the thickness dz in correspondence with the assumed representation μ_s can be expressed as μ_{bs}dz. Then, with the attenuation of the probing light on the path to the layer with the thickness dz and the attenuation of the reflected light on its path to the nearest boundary taken into account,

$$R = T_F^2 \int_0^d \mu_{bs} \exp[-2(\mu_{bs} + \mu_a) z]\, \mathrm{d}z$$

$$= T_F^2 \frac{\mu_{bs}\{1 - \exp[-2(\mu_{bs} + \mu_a)d]\}}{2(\mu_{bs} + \mu_a)}. \tag{4}$$

From expressions (3) and (4) one can derive the relation

$$\mu_{bs} = \frac{2R}{d} \frac{\ln(T_F^2/T)}{T_F^2 - T^2/T_F^2}, \tag{5}$$

and from Eqns (2), (3), and (5) the relations follow

$$\mu_a = \frac{1}{d}\ln(T_F^2/T) - \frac{2R}{d}\frac{\ln(T_F^2/T)}{T_F^2 - T^2/T_F^2}, \quad (6)$$

$$\mu_s = \frac{1}{d}\ln(T/C) + \frac{2R}{d}\frac{\ln(T_F^2/T)}{T_F^2 - T^2/T_F^2}. \quad (7)$$

Equations (6) and (7) were used by us to reconstruct the absorption (μ_a) and scattering (μ_s) spectra from the data of spectrophotometric measurements of collimated transmittance (C), full transmittance (T) and full reflectance (R).

2.3. Setup for optical diffuse spectroscopy

The experiments on the determination of optical properties of the studied objects using the ODS method were carried out with the optical diffusion tomograph (Fig. 1), designed at the Institute of Applied Physics, Russian Academy of Sciences [28]. In the used setup three small-size semiconductor lasers are located at one side of the object, their radiation being coupled out into one optical fibre at the wavelengths of 657, 802, and 919 nm (the power 13.6, 24.1, and 6.9 μW, respectively). The optical fibre face was moved parallel to the plane of the object boundary. On the phantom surface the light beam has the cross section radius $r = 1$ mm and a Gaussian intensity distribution profile. At the other side of the object a detector system is placed, based on a low-noise cooled digital ML1001E CCD camera (Finger Lakes Instrumentation, USA) and a SIGMA AF 30 F/1.4 objective, synchronised with the lasers and sequentially detecting the spatial distributions of the transmitted radiation at three abovementioned wavelengths for each position of the source. At the output of the detecting system the signal was digitised by means of a 16-bit NI USB-6251 ADC/DAC board (National Instruments, USA). The resolution of the resulting images amounts to 962 points per 1 cm^2.

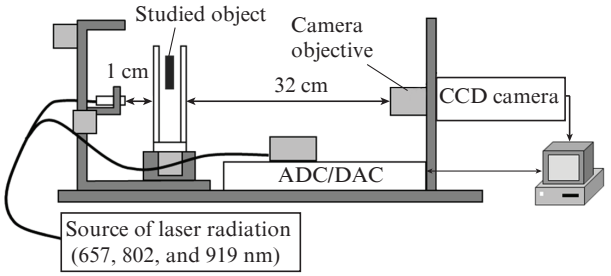

Figure 1. Schematic diagram of the setup for ODS.

3. Results

3.1. Optical properties of nanoparticle suspensions

At the first stage, based on spectrophotometric measurements the optical properties of suspensions of gold and silicon nanoparticles (Fig. 2) were reconstructed. Both in gold and silicon nanoparticles the absorption coefficient considerably exceeds the scattering coefficient, which makes it possible to consider them as contrast agents for the ODS, for which the image formation is determined mainly by the distribution of the absorption coefficient. The absorption coefficient of gold nanoparticle suspension (types 1–3) exceeds that of the silicon particles (type 4). The absorption spectra of suspensions of gold nanoparticles possess resonance features. For the particles of type 2 one can observe two maxima (so called surface plasmon resonances [17]). The first maximum at the wavelength $\lambda = 580$ nm is caused by the plasma frequency of the metal (gold), the refractive index of the surrounding medium, and the particle size, while the second maximum at $\lambda = 885$ nm is due to the presence of a fraction of nanorods with the ratio of dimensions 3 : 1 in the suspension [18]. For the particles of type 3 the maxima are observed at $\lambda = 527$ and 802 nm, respectively. For the particles of type 1 the first maximum corresponds to $\lambda = 645$ nm, while the second one, caused by the shape of the particles, is shifted into the infrared region.

Since the absorption coefficients of the nanoparticles of types 1 and 2 essentially exceed those of nanoparticles of types 3 and 4, the former were used in further experiments on contrasting the ODS images with nanoparticles.

3.2. Contrasting properties of gold nanoparticles used in ODS

Figure 3 presents the images, obtained using the ODS system at $\lambda = 802$ nm for four concentrations of Indian ink (0.01, 0.05, 0.1, and 0.5%), by which it is possible to estimate the dependence of the contrast of the selected region on the concentration of the absorber. The extinction coefficients of the phantom with the addition of Indian ink were 14.4, 15.8, 17.7, and 32.5 cm^{-1} for the considered concentrations, respectively.

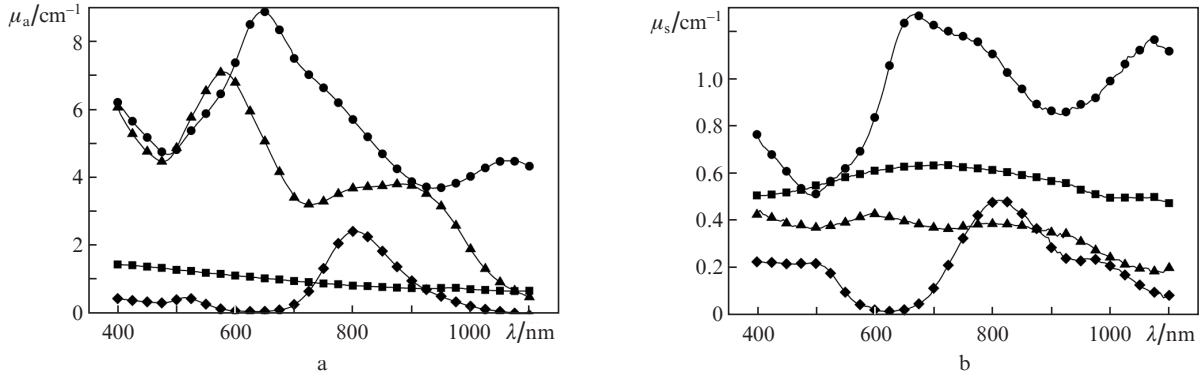

Figure 2. (a) Absorption and (b) scattering coefficients of silicon and gold nanoparticles of types (●) 1, (▲) 2, (◆) 3 and (■) 4.

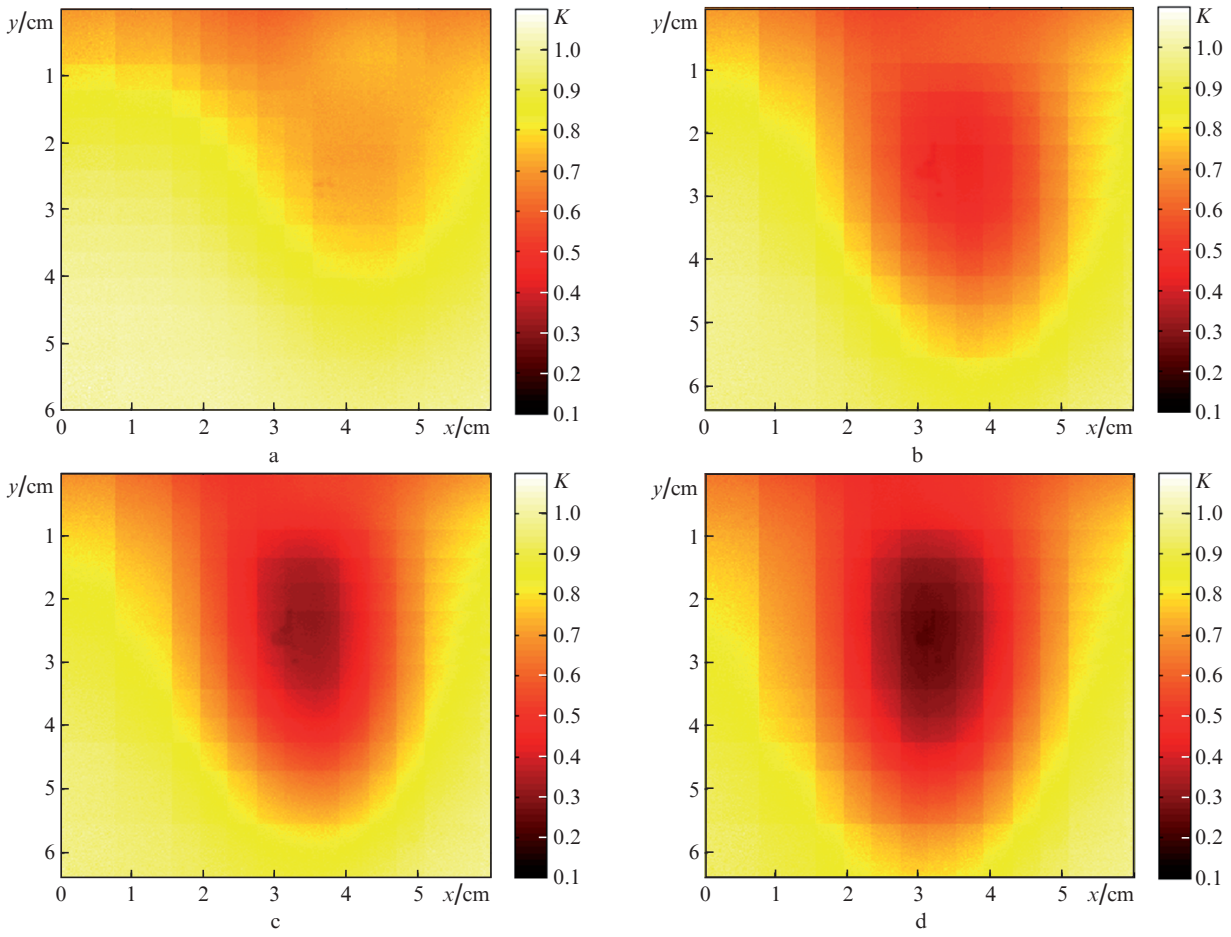

Figure 3. ODS images at $\lambda = 802$ nm for the phantom on the basis of lipofundin solution (1.4%) with the test tube, filled with the solution of lipofundin (1.4%) and Indian ink with the concentrations (a) 0.01%, (b) 0.05%, (c) 0.1% and (d) 0.5%.

The contrast of the test tube in the obtained ODS images was calculated using the formula

$$K = \frac{I_{\max} - I_{\min}}{I_{\max} + I_{\min}},$$

where $I_{\max}$ is the signal from the background medium (lipofundin solution), and $I_{\min}$ is the signal from the region corresponding to the projection of the test tube centre onto the plane of the cuvette boundary. The dependence of the selected region contrast on the Indian ink concentration and the added absorption coefficient $\tilde{\mu}_a$ is presented in Fig. 4 and exhibits an essentially nonlinear character. The range of the added absorption coefficient values agrees with the characteristics of nanoparticle suspensions of types 1 and 2.

The ODS images of the biotissue phantom with the plastic test tube before and after its labelling with gold nanoparticles of types 1 and 2 for $\lambda = 802$ nm are presented in Fig. 5, which demonstrates the contrasting of the selected region. Analogous results were obtained also for other probing wavelengths (657 and 919 nm). The quantitative estimate of the contrast of ODS images for two considered types of gold nanoparticles depending on the probing wavelength is presented in Fig. 6. It is seen that the wavelength dependence of the contrast value for both types of the considered nanoparticle suspensions agrees with the wavelength dependence of their absorption coefficient (Fi. 2,a).

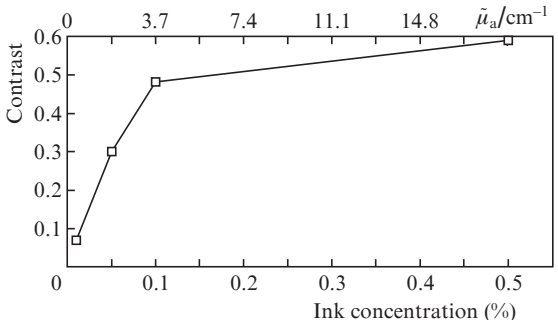

Figure 4. Dependence of the contrast of ODS images at 802 nm on the ink concentration and the corresponding added absorption coefficeint $\tilde{\mu}_a$.

4. Conclusions

In the present paper we demonstrate the possibility of contrasting the selected region in the ODS image of the optical biotissue phantom by embedding nanoparticles into it. The most efficient among the considered types of nanoparticle suspensions (gold nanoparticles of arbitrary shape with the characteristic size 30–100 nm and gold nanoparticles of arbitrary shape with a minor admixture of nanorods of length 30–50 nm and thickness 10–17 nm) were selected based on their absorption spectra, reconstructed from the spectropho-

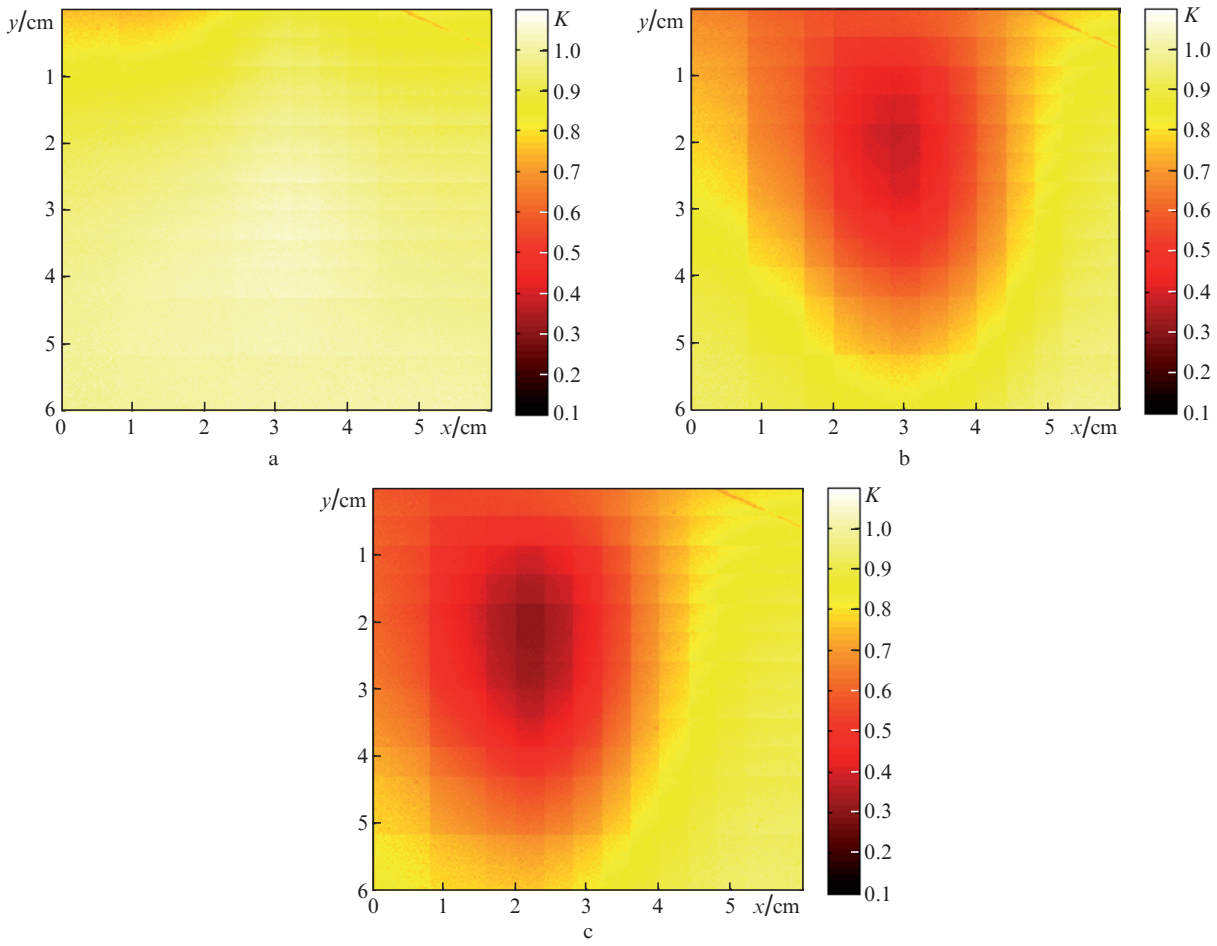

Figure 5. ODS images at $\lambda = 802$ nm of the phantom on the basis of lipofundin solutions (1.4%) with the test tube filled with the lipofundin solution (1.4%) without nanoparticles (a) and with suspension of gold nanoparticles of type 2 (b) and type 1 (c) at the extinction coefficients (a) 14, (b) 18.2 and (c) 20.9 cm^{-1}.

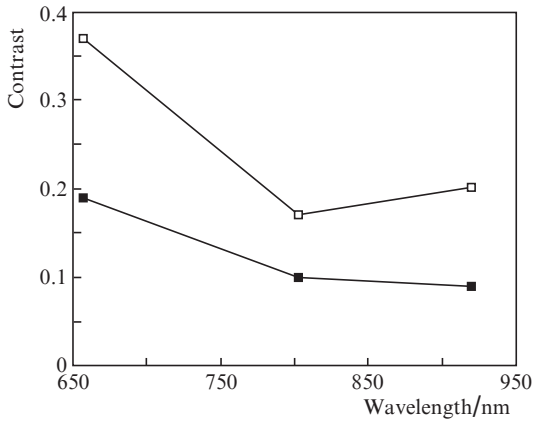

Figure 6. Contrast of ODS images for gold nanoparticles of type (□) 1 and (■) 2 vs. the wavelength.

tometry data. A specific feature of these types of nanoparticles is the essentially nonmonotonic wavelength dependence of the absorption coefficient, determined by the presence of plasmon resonances.

The experiments on contrasting the ODS images were carried out with the liquid phantom, close to the mouse biotissues in its optical properties. Calibration experiments with adding Indian ink in different concentrations to the selected region of the phantom, confined within a test tube, allowed the demonstration of essentially nonlinear dependence of the contrast on the added absorption coefficient in the selected region. The experiments with nanoparticle suspensions have shown the high potential of their employment for contrasting the selected region with the diameter 0.7 cm in the medium 4 cm thick, the wavelength dependence of the contrast value being similar to the analogous dependence of the suspension absorption coefficient.

Acknowledgements. The work was supported by the Ministry of Education and Science of the Russian Federation (Project No. 14.Z50.31.0022) and the Russian Foundation for Basic Research (Grant Nos 14-22-01086 ofi_m and 14-02-31549). The development of the ODS system was carried out within the framework of financing State Task No. 12.16 'Acoustical and Optical Methods for Studying the Structure and Dynamics of Physiological Processes in Biological Tissues'.

References

1. Tromberg B.J., Cerussi A., Shah N., Compton M., Durkin A., Hsiang D., Butler J., Mehta R. *Breast Cancer Res.*, **7** (6), 279 (2005).

2. Orlova A.G., Turchin I.V., Plehanov V.I., Shakhova N.M., Fiks I.I., Kleshnin M.I., Konuchenko N.Yu., Kamensky V.A. *Laser Phys. Lett*., **5** (4), 321 (2008).
3. Aslin R.N., Mehler J. *J. Biomed. Opt*., **10** (1), 011009 (2005).
4. Tuchin V.V. *Opticheskaya biomeditsinskaya diagnostika* (Optical Biomedical Diagnostics) (Moscow: Fizmatlit, 2007) Vol. 2, p. 109.
5. Vargas G., Chan E.K., Barton J.K., Rylander H.G., Welch A.J. *Lasers in Surgery and Medicine*, **24** (2), 133 (1999).
6. Wang R.K., Xu X., Tuchin V.V., Elder J.B. *J. Opt. Soc.Am. B*, **18** (7), 948 (2001).
7. Welzel J. *Skin Res. Technol*., **7** (1), 1 (2001).
8. Zagaynova E.V., Shirmanova M.V., Kirillin M.Yu., Khlebtsov B.N., Orlova A.G., Balalaeva I.V., Sirotkina M.A., Bugrova M.L., Agrba P.D., Kamensky V.A. *Phys. Med. Biol*., **53**, 4995 (2008).
9. Troutman T., Barton J.K., Romanowski M. *Opt. Lett*., **32** (11), 1438 (2007).
10. Au K.M., Lu Z., Matcher S.J., Armes S.P. *Adv. Mater*., **23** (48), 5792 (2011).
11. Choi J., Zheng Q., Katz H.E., Guilarte T.R. *Environ. Health Perspect*., **118** (5), 589 (2010).
12. Park J.-H., Gu L., von Maltzahn G., Ruoslahti E., Bhatia S.N., Sailor M.J. *Nat. Mater*., **8**, 331 (2009).
13. Benezra M., Penate-Medina O., Zanzonico P.B., Schaer D., Ow H., Burns A., DeStanchina E., Longo V., Herz E., Iyer S., Wolchok J., Larson S.M., Wiesner U., Bradbury M.S. *J. Clin. Invest*., **121** (7), 2768 (2011).
14. Kirillin M.Yu., Agrba P.D., Sirotkina M.A., Shirmanova M.V., Zagaynova E.V., Kamensky V.A. *Kvantovaya Elektron*., **40** (6), 525 (2010) [*Quantum Electron*., **40** (6), 525 (2010)].
15. Paciotti G.F., Myer L., Kingston D.G.I., Ganesh T., Tamarkin L. *NSTI-Nanotech*., **1**, 7 (2005).
16. Zharov V., Letfullin R.R., Galitovskaya E.N. *J. Phys. D: Appl. Phys*., **38**, 2571 (2005).
17. Gang Y., Song-You W., Ming X., Liang-Yao C. *J. Korean Phys. Soc*., **49** (5), 2188 (2006).
18. Xiaohua H., EI-Sayed Mostafa A. *J. Adv. Res*., **1**, 13 (2010).
19. Khlebtsov N.G. *Kvantovaya Elektron*., **38** (6), 504 (2008) [*Quantum Electron*., **38** (6), 504 (2008)].
20. Terentyuk G.S., Ivanov A.V., Polyanskaya N.I., Maksimova I.L., Skaptsov A.A., Chumakov D.S., Khlebtsov B.N. *Kvantovaya Elektron*., **42** (5), 380 (2012) [*Quantum Electron*., **42** (5), 380 (2012)].
21. Khlebtsov N.G., Dykman L.A. *J. Quant. Spectrosc. Radiat. Transfer*, **111**, 1 (2010).
22. Sirotkina M.A., Elagin V.V., Shirmanova M.V., Bugrova M.L., Snopova L.B., Kamensky V.A., Nadtochenko V.A., Denisov N.N., Zagaynova E.V. *J. Biophotonics*, **3** (10-11), 718 (2010).
23. Eroshova O.I., Perminov P.A., Zabotnov S.V., Gongal'skii M.B., Ezhov A.A., Golovan' L.A., Kashkarov P.K. *Kristallografiya*, **58** (6), 942 (2012) [*Crystallography Reports*, **58** (6), 831 (2012)].
24. Krainov A.D., Mokeeva A.M., Sergeeva E.A., Agrba P.D., Kirillin M.Yu. *Opt. Spektrosk*., **115** (2), 227 (2013) [*Opt. Spectrosc*., **115** (2), 193 (2013)].
25. Rogatkin D.A. *Opt. Spektrosk*., **87** (1), 109 (1999) [*Opt. Spectrosc*., **87** (1), 101 (1999)].
26. Tualle J.-M., Tinet E. *Opt. Commun*., **228** (1), 33 (2003).
27. Krainov A., Mokeeva A., Sergeeva E., Zabotnov S., Kirillin M. *Proc. SPIE Int. Soc. Opt. Eng*., **8699**, 86990Q (2013).
28. Kamensky V.A., Plekhanov V.I., Orlova A.G., Kleshnin M.S., Turchin I.V. Russian Federation Utility Model Patent No. 91517 of 20.02.2010.